Journal of Pharmaceutical and Biomedical Analysis 48 (2008) 1–7

Contents lists available at ScienceDirect

Journal of Pharmaceutical and Biomedical Analysis

journal homepage: www.elsevier.com/locate/jpba

Measuring the distribution of density and tabletting force in pharmaceutical tablets by chemical imaging

Christopher D. Ellison[a,*], Bryan J. Ennis[b], Mazen L. Hamad[a], Robbe C. Lyon[a]

[a] Division of Product Quality Research, Center for Drug Evaluation and Research, Food and Drug Administration, Silver Spring, MD 20993, United States
[b] E&G Associates, Nashville, TN 37215, United States

ARTICLE INFO

Article history:
Received 13 November 2007
Received in revised form 9 April 2008
Accepted 10 April 2008
Available online 26 April 2008

Keywords:
Compaction
Compression
Powder technology
Magnesium stearate
Density
Near-infrared imaging
Force transmission
Wall friction
Shear cell

ABSTRACT

In pharmaceutical processing, the lubricant magnesium stearate (MgS) can affect compaction efficiency based on blend time and amount of MgS used. Insufficient lubrication produces intra-tablet variations in density. Consistent tablet density profiles and uniform compaction force, as managed by proper lubrication, are important for predictable performance. The current work demonstrates the utility of near-infrared (NIR) chemical imaging in measuring density variations within compacts, and relates these variations to tabletting forces as controlled by frictional properties and quantity of MgS.

Lactose monohydrate was blended with 0%, 0.25%, or 1.0% MgS for 30 s or 30 min. Compacts were prepared of each blend, with compaction forces monitored by load cells. Frictional properties were measured by automated shear cell. NIR chemical images were collected for each tablet, and the density at each image pixel was calculated.

Density distribution within compacts was well perceived within the NIR images. Uniformity of intra-tablet density was strongly dependent upon friction between powder and die walls: tablets with no MgS or 0.25% MgS were less uniform than tablets with 1.0% MgS. In addition, absorbance variations along tablet edges, reflective of corresponding density variation, agreed with force transmission within the tablet and final tablet ejection force.

Chemical imaging techniques can be used to non-destructively assess density profiles of tablets, and confirm prediction of friction alleviation and improvement in force distribution during tabletting. The density profiles were both qualitative, showing differences in density profiles between tablets of different blends, and quantitative, providing actual density and tabletting force information within a single tablet. This work demonstrates that near-infrared chemical imaging can be an effective tool in monitoring not only the physical quality of pharmaceutical tablets, but the corresponding die forces controlling tabletting and final ejection.

Published by Elsevier B.V.

1. Introduction

During the compaction or pressing of pharmaceutical powders into tablets, the quality of the resulting tablets depends on die aspect ratio and geometry, the forces of the upper and lower punch, the speed at which this force is applied, the length of time for which the force is applied, and the powder properties of compressibility, permeability, friction and cohesion within the powder, and friction and adhesion between the powder and the die walls and punches. In particular, excessive die wall friction may promote uneven disposition of the compressive force throughout the powder, resulting in heterogeneity of density within the tablet [1,2]. For some products, dissolution rate may be affected by tablet density. In such cases, regions of greater and lesser density may impact the performance of the tablet, leading to greater variability in product performance.

The tensile strength of a tablet depends on the bonding strength between particles within the tablet. Particle size and shape can affect how particles pack together during compression, and how well the particle surfaces interact to create stronger or weaker bonds [3,4]. Under compression, brittle particles may break or shatter, while softer particles may undergo deformation to fill gaps between the particles [5,6]. The strength of the interparticulate bonds formed during compaction can be affected by the brittleness/elasticity of the material, and the rate of tablet compression [5–7]. The act of compacting powders stores energy within the tablets, by shifting or compressing the intermolecular bonds within the particles. The tablets have a natural tendency to relax once pres-

* Corresponding author. Tel.: +1 301 796 0054; fax: +1 301 796 9816.
E-mail addresses: christophe.ellison@fda.hhs.gov (C.D. Ellison), bryan.ennis@powdernotes.com (B.J. Ennis).

0731-7085/$ – see front matter. Published by Elsevier B.V.
doi:10.1016/j.jpba.2008.04.020

sure is removed, and this tendency works against the interparticle bonding formed during compression [4,5]. When stress due to this stored energy exceeds interparticle bonds, the tablet can expand, becoming more porous or even break apart. Such expansion can result in capping (when a cone-shaped core from a face of the tablet splits off spontaneously) or lamination (when one or more layers of the tablet break away) [1,4,8–10].

When friction leads to uneven compression of a tablet, there can be localized regions of increased stored energy, i.e. high stress, creating opportunities for capping and other stress-related tablet failures [1,11,12]. In addition, excessive friction and density maldistribution can lead to high ejection forces, providing additional opportunities for tablet failure during tablet expansion [1]. Magnesium stearate (MgS) is frequently used as a lubricant, having excellent ability to reduce friction between powders and die surfaces [13]. Unfortunately, MgS can reduce interparticulate bond strength, making tablets softer, more porous, and it can form a hydrophobic coating on granules during extended blending, leading to dissolution problems [14,15]. Thus it is important to use only a sufficient amount of MgS (commonly 0.25–2%, w/w), and to blend it into the powder for only a short time, usually as a last step before tabletting, or applied directly to the die to avoid blending problems.

During pharmaceutical development, and for continuous product monitoring, it would be beneficial to know that tablet density is uniform throughout a tablet. Lack of such uniformity would suggest regions of differing porosity or regions of differing stored energy, thus indicating stress-related deficiencies in product quality, and possibly poor product performance. Only a few techniques, such as indentation testing and X-ray computerized tomography (XRCT), are currently available for measuring density profiles within a tablet. Computer modeling is another approach. Discrete element computer simulations (also called "finite element models") have been effective at demonstrating the effects of die wall friction on homogeneity of density. Such simulations represent a powder bed or tablet as finely partitioned subunits which interact on one another according to the rules of a chosen model [8,9]. A popular model for simultaneous expression of elastic and plastic properties is the Drucker–Prager Cap model, which can be incorporated into discrete element models [8,9,11,13,16]. A positive feature of such material property based models is that they rely on experimentally determined yield and elastic properties as measured by indentation methods and shear cell testing [17].

Indentation testing is a classic means of measuring the hardness of materials, dating to the early 20th century. In this sense, hardness is the ability of a material to resist plastic deformation. Modern indentation testing of samples is conducted by an apparatus which applies a narrow conical tip to the sample surface under gradually increasing pressure, and measuring the impression created. For compressed powders, such as a tablet or compact, this can be correlated to density. By measuring hardness at multiple points across a tablet surface, a density map can be created for the tablet. By cross-sectioning a tablet and applying the indentation tester to the revealed section, the interior density profile can be discerned. Indentation testing has the advantages of being a direct measurement and of being a long-established method in material science. However, it is a time-consuming destructive test with low spatial resolution (only a limited number of sampling points can be measured), and making accurate measurements of indentation depth can be challenging. Recent studies have used indentation testing to calibrate/substantiate discrete element simulations [11,12].

XRCT produces a three-dimensional, high-resolution (typically 0.1–10 μm resolution) image of the physical structure of a sample. XRCT analysis of a sample consists of positioning the sample between a directed source of X-ray radiation and a detector array. The sample is rotated within the X-ray field, producing images from all angles, which are then used to produce a three-dimensional representation of the sample. Gray-scale images are related to density, and can demonstrate the heterogeneity of density within pharmaceuticals [2,18,19].

The purpose of the current work is to introduce near-infrared (NIR) chemical imaging as an alternative to indentation testing and XRCT for rapid monitoring of density profiles in tablets. NIR chemical imaging is a recently developed rapid non-destructive technique for the analysis of chemical heterogeneity in the surface layer of a sample (such as a pharmaceutical tablet). The technique has been well-described in recent literature [20–23], but is summarized here. Whereas a traditional NIR spectrophotometer produces a single spectrum to represent an entire sample, an NIR imager partitions the sample into a grid of "pixels" and provides a spectrum for each pixel. The result is a chemical map of the sample surface, showing regions of high or low drug concentration, localized presence of impurities or hydration, or the structure of more complex pharmaceutical products. NIR chemical imaging has been used to examine blending and structure in complex tablets [20,24], relate production processes to product performance [25], detect counterfeit or low-quality products [26], and quantify intra-tablet homogeneity [27].

NIR chemical imaging is nearly as fast as traditional NIR, taking only a few minutes to scan and analyze a sample, once a model has been established. However, imaging is computationally intense, and image files are large (10–100 MB), so only with recent advances in computer technology has the method become practical. File size depends on a combination of spatial and spectral resolution. Spatial resolution for NIR chemical imaging is typically 10–200 μm per pixel. Spectral resolution (the step-size between measured near-infrared wavelengths) of 10 nm is commonly used to keep file size manageable, and much better spectral resolution is available if necessary. Though imaging is not a three-dimensional technique like XRCT, maps of the internal structure can be obtained by sectioning the sample and analyzing the revealed surface, as with indentation analysis.

A confounding factor in NIR analysis (traditional or imaging), is that physical properties, including density, hardness, and particle size, have an impact on the spectrum, typically a linear baseline shift [28,29]. Such changes in the physical properties of a material can alter the pathlength of the incident illumination as it is refracted and reflected by particle surfaces in the surface layers of the sample. A longer pathlength provides more absorbance, and provides greater intensity across the spectrum. This impact is often minimized by various chemometrics preprocessing steps, including multiplicative signal correction or Savitzky–Golay differentiation. Rather than eliminate this baseline shift, the current study analyzes it to examine density changes along the surface of a tablet.

NIR spectra have been correlated to particle size for powders, or in the case of tablets, to initial (pre-compaction) particle size. Vromans et al. [30] has demonstrated that for lactose monohydrate, densification depended on initial particle size, so it makes sense that if NIR can be related to density, it can also be related to initial particle size. For brittle particles, such as lactose monohydrate, fragmentation is an important part of compaction, and density variations likely indicate differences in final (compacted) particle sizes, though we are unaware of any direct demonstrations of this. It would be difficult to divorce the effects of final particle size and tablet density for such materials. Density and particle size are not closely related for other materials, however, since many materials undergo plastic deformations during compaction, forming a denser tablet without any fragmentation.

A model system, lactose blended with varying amounts of MgS, was selected for this study. The forces transmitted through the tablets and the losses due to wall friction were measured during

compression by a custom designed apparatus using standard compression load cells. It was expected that the addition of MgS would reduce powder friction in the blend and losses due to wall friction, allowing compression forces to be transmitted more uniformly throughout the tablet. Measurements of powder and wall friction and adhesion were made by automated rotary shear cell [1]. The variation in MgS content in the blends resulted in variation in tablet density profiles. Chemical imaging was used to evaluate intra-tablet density distribution, and was contrasted with tabletting and ejection forces as well.

2. Materials and methods

Lactose monohydrate (Type 316, "Fast-Flo") was obtained from Foremost Farms (Baraboo, WI). MgS (puriss grade) was obtained from Sigma–Aldrich/Riedel-de Haën (Seelze, Germany). Lactose was blended with MgS (0.25% or 1.0%, w/w) using a Turbula T2F orbital shaker (Glen Mills, Inc., Clifton, NJ) at 72 cycles/min for 30 s or 30 min.

Compacts (300 mg) of pure lactose and each blend were formed using a benchtop hydraulic press (Carver model 3889, Wabash, IN) at 2000 lb, 40% pump speed, 1 min dwell time with a (3/8) in. diameter stainless steel cylindrical punch and die set (The Elizabeth Companies, McKeesport, PA) (Fig. 1). A custom-made holder utilizing compression load cells was positioned under the lower (non-moving) punch and under the die support ring during tabletting to record transmitted forces (Fig. 1). Specifically, for a given applied force to the upper punch, the load cell under the lower punch recorded the force transmitted directly through the powder bed, and the load cell under the die recorded the force conveyed to the die by friction between powder and the interior die wall. Following compression, the die was flipped horizontally, the upper punch was reinserted, and the tablet ejection force was measured. The top/bottom orientation of each compact was carefully maintained after tabletting and ejection.

Powder flow measurements were conducted by an iShear™ automated rotary split shear cell (iPowder Systems, Nashville, TN). A sample of powder is contained in a cell consisting of a ring and base (or ring and wall surface in the case of wall friction measurements) [1]. The cell is sheared in rotation, forming a shear plane between the upper and lower halves of powder. In the case of wall friction, the powder half is sheared against a polished stainless steel coupon. The torque required to shear the cell, or the shear stress, is measured as a function of applied compressive force (or normal stress.) Both the effective angle of powder friction, and a wall friction angle may be determined, in addition to wall adhesion and powder cohesion. Additional discussion of these measurements and their impact on tabletting forces as measured by the load cell assembly will be discussed in greater detail in a future publication.

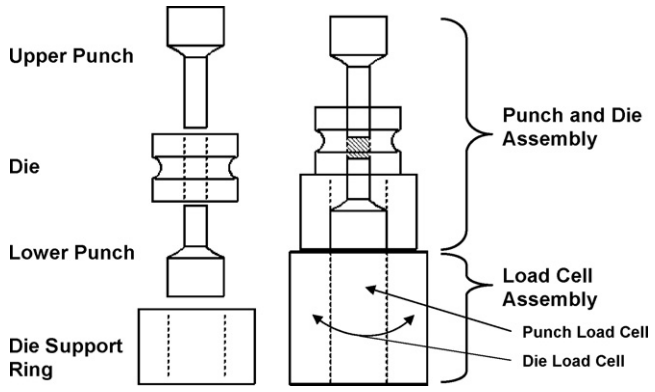

Fig. 1. Profile view of cylindrical punch and die set. A pair of concentric load cells is positioned beneath the punch-and-die assembly within the hydraulic press. The central load cell monitors force transmitted through the powder to the bottom punch, and the outer load cell monitors force lost to the die wall via friction.

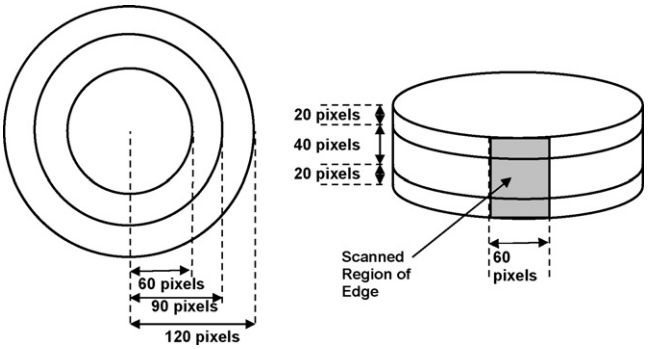

Fig. 2. For analysis, top and bottom tablet images were divided into concentric rings, and the average absorbance for each ring computed. The tablet edge was divided into the top quarter, the bottom quarter, and the center.

Tablet surfaces (tops and bottoms) and edges were imaged using a Sapphire Near-Infrared Chemical Imaging System (Spectral Dimensions, Olney, MD), 1400–2450 nm at 10 nm steps, each measuring the average of eight "coadds." Spatial resolution was 39 μm per pixel, 256 × 320 pixels per image. Raw reflectance images were standardized against zero-reflectance and high-reflectance standards, then transformed to absorbance images by $A = \log(1/R)$. For density analysis, the absorbance image at the single wavelength, 2120 nm, was selected. Because the compacts are pure (or nearly pure) lactose, no spectral changes due to chemical variability are expected, only a linear shift in the baseline, which suggests a univariate analysis rather than more complex techniques such as PCA or PLS. The shift is related to absorbance, making peaks in the lactose spectrum good choices for enhancing differences. Clarke et al. published an excellent review of NIR penetration, and demonstrated that when imaging, lower wavelengths (1100 nm) obtain information from as deep as 777 μm, while higher wavelengths (2500 nm) penetrate approximately one-seventh as deeply [31]. The results of Clarke et al. [31] would vary based on chemical and physical properties of the sample, but indicate that a longer wavelength is desirable to avoid excessive penetration and averaging of the resulting signal. The chosen wavelength meets these criteria.

A model correlating NIR spectra to density of lactose compacts was generated by comparing whole-tablet densities to average absorbance at 2120 nm. The whole-tablet density of a compact was measured directly as the ratio of mass and volume. The average absorbance at 2120 nm for a compact was calculated as the mean absorbance at all top and bottom pixels of the compact's images. Compacts used in calibrating the model included those previously described and additional compacts produced at 1000 lb and 4000 lb pressure. The model was applied to each pixel of the studied compacts to generate local density values. Additionally, the average density was calculated for different regions of the compacts (Fig. 2). For tops and bottoms, the circular images were divided into outer, middle, and inner rings as described in Fig. 2. For the edges, each image was divided into three bands: the top 25%, middle 50%, and bottom 25%. The average density for each region was computed.

3. Results and discussion

Load cell data collected during tabletting of lactose compacts with 0% and with 1% MgS are displayed in Fig. 3. The "steps" in these force plots are due to adjustments made by the Carver Press to maintain 2000 lb of total force. In a frictionless system, all of

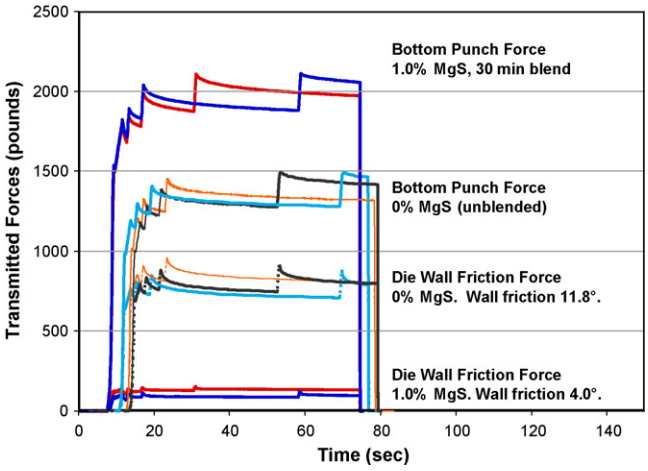

Fig. 3. Load cell measurements of compressive force transmitted through the powder to the lower punch, and to the die (via friction) is displayed for 0% and 1% MgS (30 min blend) samples. The "steps" in these force plots are due to adjustments in pressure made by the Carver Press to maintain 2000 lb pressure. Wall friction angles measured by iShear split cell against a stainless steel coupon of mirror finish.

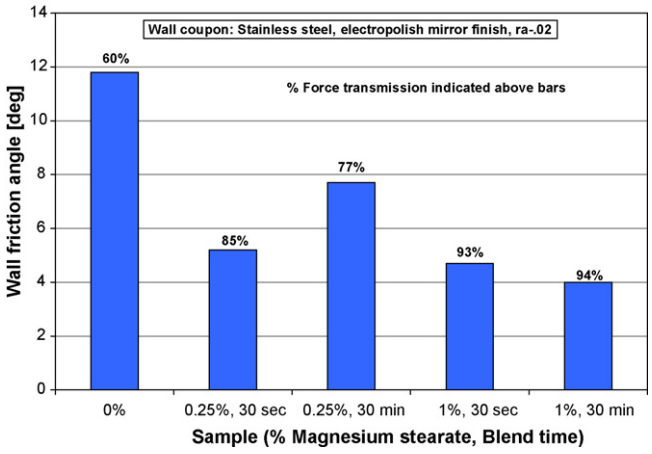

Fig. 4. Wall friction angles for lactose samples blended with MgS, as measured by iShear rotary split cell against a stainless steel coupon of mirror finish (electropolished, Ra = .02).

that force would be transmitted through the powder to the lower punch, and recorded by the load cell under the punch. Furthermore, there would be uniform pressure throughout the powder bed (gravity effects are negligible compared to the applied force), and the powder would be compacted until it has the strength to resist the pressure. The final density of the compacted tablet would likewise be uniform.

Friction does, however, occur between the lactose and the die wall. A fraction of the force applied to the powder is realized as radial stress normal to the die wall. Friction between the powder and the die wall is directly proportional to the radial stress. The ratio of wall shear stress to radial stress is the coefficient of friction, i.e. the tangent of the wall friction angle. This friction allows a portion of the applied force to be resisted by the die wall, so less of the force is transmitted deeper into the powder bed, and even less reaches the bottom of the powder bed, to be recorded by the bottom punch load cell. As the force transmitted through the powder decreases with depth, so does the correlating pressure and resultant densification. As described in Section 2, a second load cell was used to measure die wall friction force, i.e. the force transmitted to the die.

The impact of die wall friction on the compaction of the tablet is most apparent near the die wall. For tablets with high aspect ratio (diameter/thickness), there may be little impact of the wall friction on the center part of the tablet. For the current tablets (9.6 mm diameter, 3.2 to 3.9 mm thickness), wall friction had a significant impact on the density profiles of the tablets, as demonstrated below.

For pure lactose in the absence of lubricant, 36% of the compression force (720 lb) was transmitted, or lost, to the die walls due to friction. This indicates that the powder at the bottom of the die was under far less pressure than the powder at the top of the die, inducing a difference in density throughout the final compact. Lactose blended with 1% MgS for 30 min experienced only 5% loss of pressure to the die walls (Fig. 3). In contrast to the former case, this indicates that the pressure was nearly uniform throughout the powder bed during compaction, suggesting a uniformly dense final compact. Furthermore, this comparison demonstrates that the inclusion of MgS significantly reduces die wall friction, as expected, and impacts the density profile of the produced compacts. This is verified by a drop in measured wall friction angle from 11.8° for pure lactose to 4.0° for lactose blended with 1% MgS (Fig. 4).

As illustrated in Fig. 5, the spectra within a nearly pure compact can vary due to physical rather than chemical differences. Density differences are reflected by a baseline shift in NIR, rather than a qualitative spectral change. To observe this shift, a single wavelength (2120 nm) was chosen. The choice avoids the sometimes variable water peak at 1940 nm and the noisy region at 2400 nm. Derivatives, normalization, and other forms of preprocessing minimize the impact of physical characterization in order to highlight chemical differences. Thus, analysis was performed on the absorbance data without preprocessing.

Fig. 6 shows representative tablet images from each blend: lactose monohydrate with 0%, 0.25%, or 1% MgS, blended for 30 s or 30 min, and pressed at 2000 lb. The images are displayed in the same scale, based on absorbance at 2120 nm. The top row shows the tops of each compact, the middle row shows the edges, and the

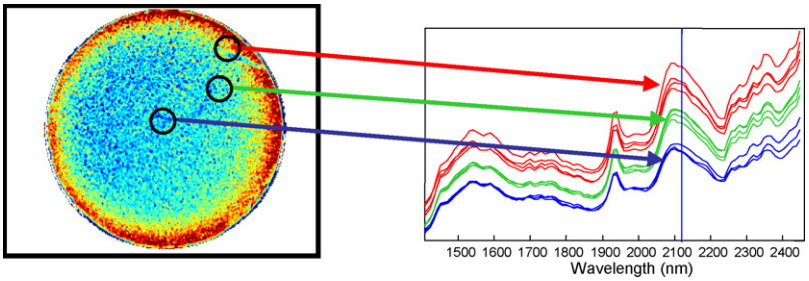

Fig. 5. This absorbance image of a pure-lactose compact demonstrates how each point ("pixel") on the compact's surface generates a spectrum. The colors in this image are based on absorbance level at 2120 nm. (For interpretation of the references to color in this figure legend, the reader is referred to the web version of the article.)

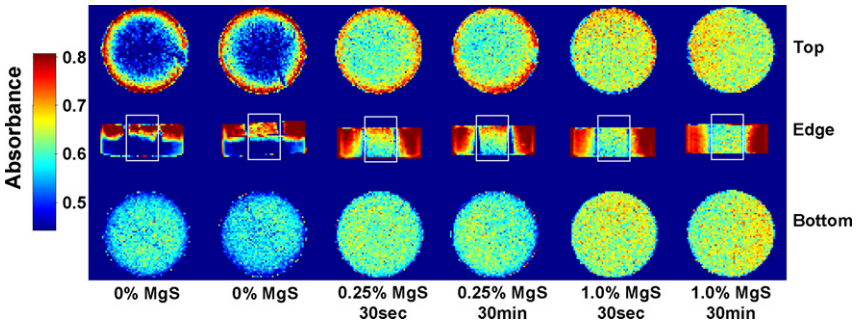

Fig. 6. Comparison of tablet absorbance profiles. Representative images of tablet tops, bottoms, and edges are shown for 0%, 0.25%, and 1.0% MgS blended 30 s or 30 min. Higher absorbance correlates to higher density.

lower row shows the bottoms of each compact. The tablet edges of these circular compacts curve away from the imager's lens, out of the field of focus. The center of the image, a region 60 pixels (nearly 2.5 mm) wide, is well focused, so only the central portion of the edge image is considered for analysis (cf. Fig. 2). These images allow for an immediate qualitative assessment of differences in the compacts, based on density distribution. The compacts with 0% MgS show extreme internal density variations, while those with 0.25% show less variation, and with 1.0% MgS, only minimal variability of density is apparent. Differences in the images seem primarily related to the amount of MgS. The impact of blend time for these fast flow lactose samples depends on stearate level, discussed in greater detail below.

To assess the density at each pixel quantitatively, a calibration curve was generated based on the measured densities of 24 lactose compacts and their average absorbance at 2120 nm, as determined as an average of all pixels on the tops and bottom surfaces of those compacts (Fig. 7). Such an approach presumes that the density gradient from top to bottom of the tablet is linear, which is not likely, since pressure decreases exponentially. This decrease is, however, approximately linear ($R^2 > 0.99$) until the pressure is reduced by 50%. As previously indicated, the reduction in the current work is at most 36%, well within the linear range. The data yields a best-fit exponential calibration curve ($R^2 = 0.9905$):

$$D = 1.4 - 21.16\,e^{-8.41A}$$

where D is density in mg/cm^3 and A is absorbance at 2120 nm.

The images were divided into regions (see Fig. 2), and the average absorbance for each region was calculated and converted to density based on the above equation (Fig. 8 shows the results for the 30 min blends). With 1% MgS, there is little change in density throughout the compacts. For the compacts with 0.25% MgS, there is slightly higher density in the outer ring of the upper surface, and slightly lower density in the outer ring of the lower surface. For these compacts, there is a clear density gradient on the edge of the compact, as also illustrated in Fig. 9. This effect is greatly pronounced in the compacts with no MgS, in which the outer ring of the top surface had much greater density than the rest of the compact. In this case, the edge of the compact shows a sharp delineation between dense and non-dense regions, with delamination visible in the chemical images shown in Fig. 6. Note that linear fits to the individual data sets of the pure lactose tablet intersect at the delamination point, as shown in Fig. 9.

The higher density in the top edge of the poorly lubricated compacts is as expected, based on the literature. As the punch compresses the powder, friction between the unlubricated powder and the die wall resists powder motion, causing the localized compaction rather than transference of the pressure and more general compaction. The press used in this work has a fixed bottom platen and a moving upper punch. It is expected that if a press compresses from both directions simultaneously, a ring of high density could be formed on top and bottom of the resulting tablets or compacts, with a lower density core.

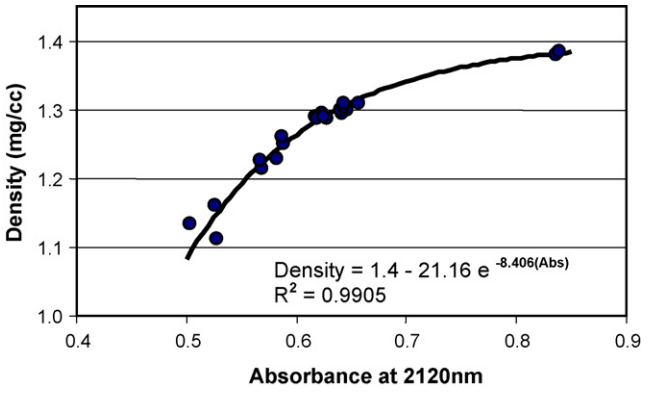

Fig. 7. Calibration model of lactose density vs. absorbance at 2120 nm. The curve is based on direct mass and volume measurements of 24 lactose (with or without MgS) compacts generated under 1000–4000 lb pressure.

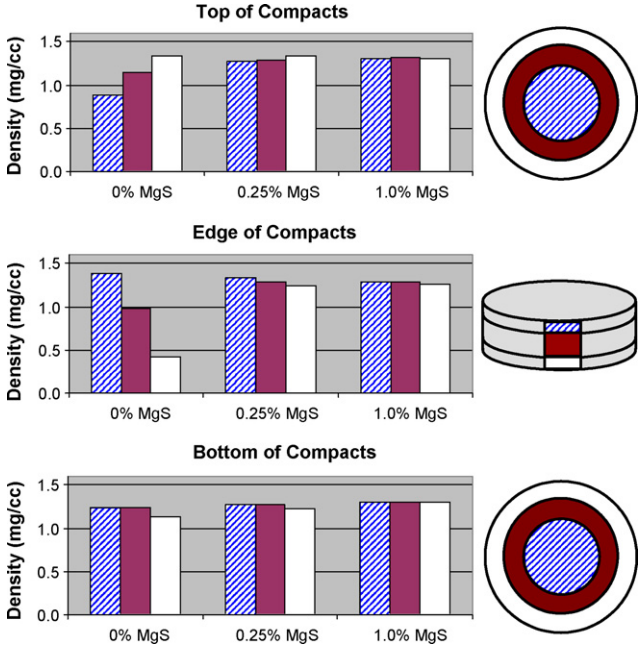

Fig. 8. Density profiles of lactose compacts. The density model equation (Fig. 7) is applied to the lactose compact images (Fig. 6), according to the defined regions (Fig. 2) of each compact. Results for the 30 min blends are displayed.

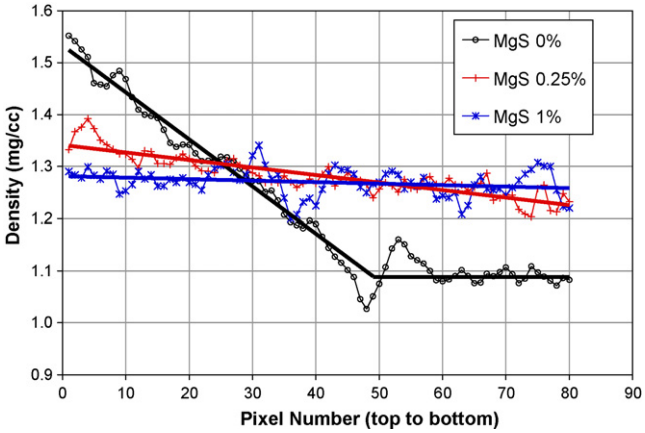

Fig. 9. Top to bottom density profiles taken along the edge of lactose tablets by pixel. Linear fits indicated by line. For delaminated tablets two linear fits were used, above and below the break.

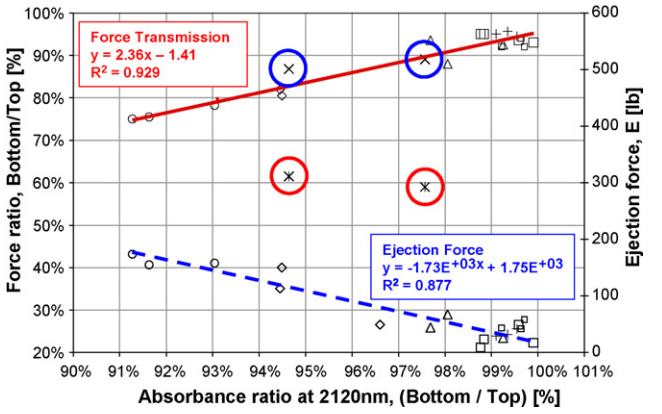

Fig. 11. Comparison of the ratio of average absorbance measured on the top and bottom tablet surface to the ratio of punch forces (or stress transmission) (left axis), and to the maximum required tablet ejection force (right axis). The outliers (circled) are lactose samples without MgS.

The absorbance profiles of the tablets may also be compared to the pressures developed during compression and subsequent die ejection. In Fig. 10, the average absorbance of the top and bottom faces are shown to be a linear function of relevant powder pressure during compression, i.e. at either upper or lower punch interface. Data from delaminated (cracked) tablets are shown in Fig. 10, circled, but are not included in the correlation. The correlation of absorbance to pressure at the top punch interface is nearly identical to the correlation at the bottom punch interface, suggesting that the mechanism of compaction is similar at top and bottom of the powder bed.

The loss in compaction force due to die wall friction may be characterized by a stress or force transmission ratio, taken as the ratio of the lower punch force to the applied upper punch force. In similar fashion, we may take the ratio of average absorbance measured on the lower to top tablet face, as a measure of density uniformity resulting from the compaction forces. A clear linear relationship between this absorbance ratio and the force transmission ratio is indicated in Fig. 11 (left axis data, upper curve).

As shown in Fig. 11, tablet ejection force also correlates with absorbance ratio (right axis), lower curve, with increasing absorbance ratio (i.e. better force transmission, and more uniform density). High die wall friction leads to low stress transmission, with the majority of compressive force being located near the upper punch. This results in high residual radial forces acting on the die wall after load removal, leading in turn to high ejection force.

The proposed method for estimating density using NIR chemical imaging is best applied to products with flat or nearly flat surfaces. Many modern pharmaceuticals are rounded or beveled on top and bottom, or include scores and imprints, which can present challenges to the proposed technique. In the current study, the edges of circular tablets were studied (Fig. 6, middle row; and Fig. 12). It is clear that the quality of the data degrades as the sample surface curves away from the lens of the imager. Specifically, high reflectance regions (the vertical blue stripes in Fig. 12a) occur where the angle of incident NIR approximately equals the angle of reflection from the sample surface to the lens; that is, where the tablet edge is at an angle of 20–26° (see Fig. 12b). These angles were calculated by applying standard trigonometric functions to the image. The central portion of this image was useful for determining the

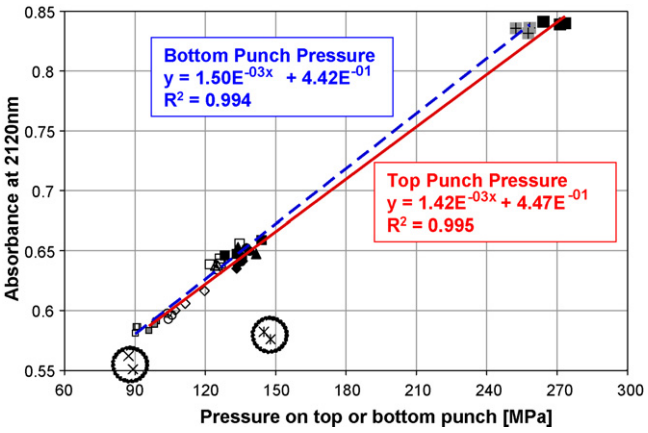

Fig. 10. Comparison of the total tablet average absorbance to measured pressure. The bottom punch force was measured directly, and the total upper punch force taken as the sum of load cell forces. Pressure was calculated based on 9.60 mm diameter punch. Linear fits to upper punch and lower punch include only samples with MgS. The outliers (circled) are lactose samples without MgS.

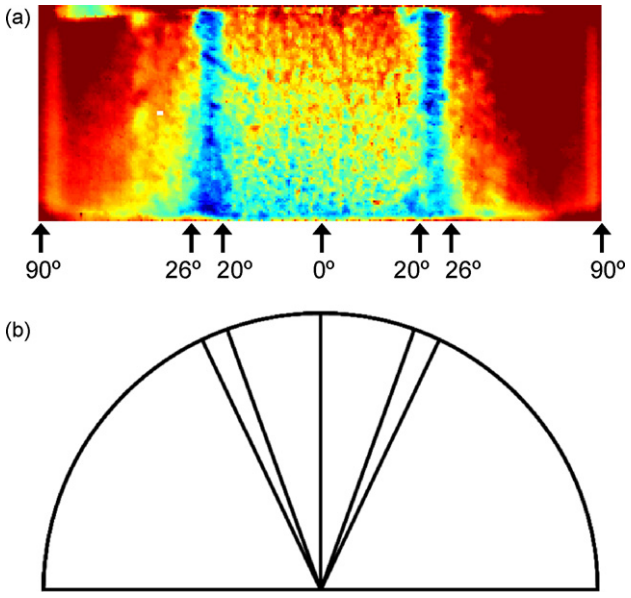

Fig. 12. (a) Absorbance profile of a tablet edge. This lactose tablet (0.25% MgS) shows reduction of image quality as the round tablet curves away from horizontal. From 20° to 26° a high reflectance region occurs where the angle of incident NIR illumination equals the angle of reflectance directly to the instrument's detector. (b) Depiction of critical angles, as determined in (a).

distribution of density. Altering the placement of the NIR illumination sources may extend this limit. Many products with rounded top and bottom have a flat regions (e.g., the edges of caplets) which can be sampled for density variations, or have sufficiently flat regions that can be presented to the instrument at an oblique angle to improve data capture. Certainly flat tablets produced during product design could be tested to ensure appropriate lubrication. Future work can examine this process as applied to heterogeneous tablets, commercial products, and cross-sections.

4. Conclusion

This work demonstrates that near-infrared chemical imaging can be an effective tool in monitoring not only the physical quality and uniformity of pharmaceutical tablets, but also as a tool to monitor the uniformity of the stresses which actually control compaction and subsequent tablet ejection. Specifically, a method was demonstrated for using imaging to produce density profiles for compacts of lactose monohydrate with differing amounts of lubricant. The density profiles are both qualitative, showing differences in density profiles between tablets of different blends, and quantitative, providing actual density information within a single tablet, which was also shown to correlate with upper and lower punch forces. For this analysis, it was important to demonstrate that the chosen lubricant levels provided a range of friction, as was indicated by load cell and shear cell data. This imaging technique could be utilized for determining an appropriate lubricant level for a new pharmaceutical, for monitoring the quality of tablets in an existing process, or for comparing the efficiency of different lubricants. In addition to being a rapid, non-destructive, high-resolution technique for density profiling, the method also has the potential to simultaneously provide information on chemical heterogeneity, impurities, hydration, and other chemical information.

References

[1] B.J. Ennis (Ed.), Perry's Chemical Engineers Handbook, 8th ed., McGraw Hill, 2007.
[2] J.J. Lannutti, MRS Bull. 22 (1997) 38–44.
[3] C. Gustafsson, C. Nyström, H. Lennholm, M.C. Bonferoni, C.M. Caramella, J. Pharm. Sci. 92 (2003) 460–470.
[4] K. Van der Voort Maarschalk, K. Zuurman, H. Vromans, G.K. Bolhuis, C.F. Lerk, Int. J. Pharm. 140 (1996) 185–193.
[5] K.M. Picker, Pharm. Dev. Technol. 6 (2001) 61–70.
[6] M. Duberg, C. Nyström, Powder Technol. 46 (1986) 67–75.
[7] R.J. Roberts, R.C. Rowe, J. Pharm. Pharmacol. 37 (1985) 377–384.
[8] C.-Y. Wu, O.M. Ruddy, A.C. Bentham, B.C. Hancock, S.M. Best, J.A. Elliott, Powder Technol. 152 (2005) 107–117.
[9] C.-Y. Wu, B.C. Hancock, A. Mills, A.C. Bentham, S.M. Best, J.A. Elliott, Powder Technol. 181 (2008) 121–129.
[10] K. Van der Voort Maarschalk, K. Zuurman, H. Vromans, G.K. Bolhuis, C.F. Lerk, Int. J. Pharm. 151 (1997) 27–34.
[11] I.C. Sinka, J.C. Cunningham, A. Zavaliangos, J. Pharm. Sci. 93 (2004) 2040–2053.
[12] I.C. Sinka, J.C. Cunningham, A. Zavaliangos, Powder Technol. 133 (2003) 33–43.
[13] W.A. Strickland Jr., T. Higuchi, L.W. Busse, J. Am. Pharm. Assoc. 49 (1960) 35–40.
[14] K. Zuurman, K. Van der Voort Maarschalk, G.K. Bolhuis, Int. J. Pharm. 179 (1999) 107–115.
[15] W.A. Strickland Jr., E. Nelson, L.W. Busse, T. Higuchi, J. Am. Pharm. Assoc. 45 (1956) 51–55.
[16] J.C. Cunningham, I.C. Sinka, A. Zavaliangos, J. Pharm. Sci. 93 (2004) 2022–2039.
[17] R.W. Lewis, R.S. Ransing, D.T. Gethin, Casting and Powder Compaction Group, Department of Mechanical Engineering, University of Wales Swansea, http://www.swan.ac.uk/nfa.
[18] B.C. Hancock, M.P. Mullarney, Pharm. Technol. 29 (2005) 92–100.
[19] I.C. Sinka, S.F. Burch, J.H. Tweed, J.C. Cunningham, Int. J. Pharm. 271 (2004) 215–224.
[20] R.C. Lyon, D.S. Lester, E.N. Lewis, E. Lee, L.X. Yu, E.H. Jefferson, A.S. Hussain, AAPS PharmSciTech 3 (2002), Article E17.
[21] F.W. Koehler IV, E. Lee, L.H. Kidder, E.N. Lewis, Spectrosc. Eur. 14 (2002) 12–19.
[22] G. Reich, Adv. Drug Deliv. Rev. 57 (2005) 1109–1143.
[23] Y. Roggo, A. Edmond, P. Chalus, M. Ulmschneider, Anal. Chim. Acta 535 (2005) 79–87.
[24] R.C. Lyon, E.H. Jefferson, C.D. Ellison, L.F. Buhse, J.A. Spencer, M.M. Nasr, A.S. Hussain, Am. Pharm. Rev. 6 (2003) 62–70.
[25] Y. Roggo, N. Jent, A. Edmond, P. Chalus, M. Ulmschneider, Eur. J. Pharm. Biopharm. 61 (2005) 100–110.
[26] B.J. Westenberger, C.D. Ellison, A.S. Fussner, S. Jenney, R.E. Kolinski, T.G. Lipe, R.C. Lyon, T.W. Moore, L.K. Revelle, A.P. Smith, J.A. Spencer, K.D. Story, D.Y. Toler, A.M. Wokovich, L.F. Buhse, Int. J. Pharm. 306 (2005) 56–70.
[27] M.L. Hamad, C.D. Ellison, M.A. Khan, R.C. Lyon, J. Pharm. Sci. 96 (2007) 3390–3401.
[28] J.D. Kirsch, J.K. Drennen, J. Pharm. Biomed. Anal. 19 (1999) 351–362.
[29] K.M. Morisseau, C.T. Rhodes, Pharm. Res. 14 (1997) 108–111.
[30] H. Vromans, A.H. De Boer, G.K. Bolhuis, C.F. Lerk, Acta Pharm. Suec. 22 (1985) 163–172.
[31] F.C. Clarke, S.V. Hammond, R.D. Jee, A.C. Moffat, Appl. Spectrosc. 56 (2002) 1475–1483.